

## Spatiotemporal chaos in the one-dimensional complex Ginzburg–Landau equation

B.I. Shraiman,<sup>a</sup> A. Pumir,<sup>b,c</sup> W. van Saarloos,<sup>a,d</sup> P.C. Hohenberg,<sup>a</sup> H. Chaté<sup>a,c</sup>  
and M. Holen<sup>a,f</sup>

<sup>a</sup>AT&T Bell Laboratories, Murray Hill, NJ 07974, USA

<sup>b</sup>Dept. of Physics, Cornell University, Ithaca, NY 14853, USA

<sup>c</sup>Laboratoire de Physique Statistique, ENS, Paris, Cedex 05, 75231, France

<sup>d</sup>Instituut Lorentz, University of Leiden, 2311 SB Leiden, The Netherlands

<sup>e</sup>Service de Physique de l'Etat Condensé, CEN Saclay, 91191 Gif-sur-Yvette, France

<sup>f</sup>Department of Mathematics, Princeton University, Princeton, NJ 08544, USA

Received 3 September 1991

Revised manuscript received 3 March 1992

Accepted 4 March 1992

Communicated by H. Flaschka

The dynamical behavior of a large one-dimensional system obeying the cubic complex Ginzburg–Landau equation is studied numerically as a function of parameters near a supercritical bifurcation. Two types of chaotic behavior can be distinguished beyond the Benjamin–Feir instability, a phase turbulence regime with a conserved phase winding number and no phase dislocations (space-time defects), and a defect regime with a nonzero density of defects. The transition between the two can either be continuous or discontinuous (hysteretic), depending on parameters. The spatial decay of the phase correlation function is inferred to be exponential in both regimes, with a sharp decrease of the correlation length upon entering the defect phase. The temporal decay of correlations is exponential in the defect regime.

### 1. Introduction

While there has been considerable progress in our understanding of the chaotic dynamics of dissipative systems involving a small number of degrees of freedom [1], there remains a challenging question, and one of considerable experimental relevance, concerning the behavior of spatially distributed systems with many active degrees of freedom. This situation is encountered whenever the “energy injection” scale is considerably smaller than the “lateral” size of the system. It has been suggested [2] that chaotic behavior in the limit of an infinite system, i.e. *extensive* chaos, might be understood in terms of concepts derived from statistical mechanics and critical phenomena. With this goal in mind, in the present work we study the chaotic behavior

of a simple model, the complex Ginzburg–Landau equation in one dimension [3–5]

$$\partial_t A = A + (1 + ic_1) \partial_x^2 A - (1 - ic_3) |A|^2 A, \quad (1)$$

on a domain  $0 \leq x \leq L$  with periodic boundary conditions and  $L$  chosen large enough to approximate the infinite system ( $L \sim 10^3$ ). Eq. (1) displays a variety of regimes in different regions of parameter space<sup>#1</sup>. In particular, for  $c_1 = c_3 = 0$

<sup>#1</sup>The minus sign in front of the nonlinear term in eq. (1) corresponds to a supercritical bifurcation. More generally, if we write eq. (1) as  $\partial_t A = A + (1 + ic_1) \partial_x^2 A - g(1 - ic_3) \times |A|^2 A$ , we may always choose scales such that  $c_1 > 0$  and  $g^2 = 1$ , and a natural extension of the phase diagram of fig. 3 is in terms of the parameters  $c_1$  and  $gc_3$ , both of which may change sign. For  $gc_3 > 0$ , the quadrant with  $c_1 < 0$  was considered by Bretherton and Spiegel [4], whereas for  $gc_3 < 0$ , (corresponding to a subcritical bifurcation) the quadrants with  $c_1 > 0$  and  $c_1 < 0$  have recently been studied by Schöpf and Kramer [5].

the dynamics is purely relaxational, while the  $c_1, c_3 \rightarrow \infty$  limit corresponds to the integrable nonlinear Schrödinger equation [3]. For  $c_1 c_3 < 1$ , eq. (1) possesses linearly stable plane-wave solutions,  $A = a_k e^{i(\omega_k t + kx)}$ , with  $a_k^2 = 1 - k^2$  and  $\omega_k = c_3 - (c_3 + c_1)k^2$  in a band of wavevectors  $|k| \leq k_{\max}(c_1, c_3)$  which shrinks to zero along the line  $c_1 c_3 = 1$ , corresponding to the Benjamin–Feir [6] (BF or modulational) instability of the uniform ( $k = 0$ ) oscillatory state [3]. Coexisting (in the parameter space) with plane waves are more complex wavetrains, corresponding to (small) local modulations of the wavenumber, and small adiabatic readjustments of the amplitude [7]. All these steady states are classified by an integer winding number

$$\nu = (2\pi)^{-1} \int_0^L \partial_x \phi(x, t) dx,$$

where  $\phi$  is the phase of  $A$ .

The present paper is mostly concerned with a study of the phase diagram for  $c_1 c_3 \geq 1$  and  $c_1, c_3 \sim O(1)$ . We find that beyond the BF instability, the system enters a “phase turbulent” regime similar to that of the Kuramoto–Sivashinsky (KS) equation [8] (or its generalization [7] appropriate to  $\nu \neq 0$ ), followed by a more strongly chaotic regime involving large-amplitude fluctuations and “phase defects” as will be discussed in some detail below. Curiously, the number of coexisting attractors, or alternatively the dependence of the asymptotic behavior on the initial conditions, appear to decrease as  $c_1 c_3$  increases beyond the BF instability.

In the present paper we have not attempted to systematically explore *all* of the attractors of eq. (1) for  $c_1 c_3 \geq 0$ , but have rather concentrated on quantitative characterizations of the chaotic states and on the transition from KS-like weak phase turbulence to defect chaos. The two are distinguished by the presence of a finite density of phase dislocation events (here called “space-

time defects”) in the latter state. These defects, which occur when  $A$  goes through zero locally, allow the winding number  $\nu$  to change<sup>#2</sup>. In contrast, in the KS (phase turbulent) state, the density of defects vanishes, at least to within our numerical resolution, making the winding number  $\nu$  a constant of the motion. We have thus confined our study of the phase turbulent states to those in the  $\nu = 0$  sector. We find that as  $c_1$  decreases the transition between phase and defect chaos changes from continuous to discontinuous at a particular point in the  $(c_1, c_3)$  plane, below which there is a hysteretic (“bichaotic”) region.

Besides a numerical calculation of the defect density  $n_D$ , we have attempted to characterize phase and defect chaos quantitatively by measuring correlation functions in space and time. The spatial correlation functions are found to decay exponentially in the defect chaos regime, while in the phase chaos region the correlation length is very long (close to the limits of our numerical resolution) and the exponential decay of spatial correlations is inferred indirectly. Temporal correlations in the defect chaos regime also decay exponentially, while in the phase turbulent state we have observed long-time correlations of long-wavelength modes, indicative of diffusive or subdiffusive relaxation. Although a number of studies of the chaotic dynamics of the Ginzburg–Landau model (1) in large systems have been undertaken since the pioneering paper of Bretherton and Spiegel [4], and in particular the transition from phase turbulence to defect turbulence was recently noted by Sakaguchi [9], we believe that ours is the first attempt at a systematic study of the phase diagram of eq. (1) in the  $(c_1, c_3)$  plane, and at a quantitative description of the chaotic states in terms of correlation functions.

<sup>#2</sup>The space-time defects discussed here should not be confused with vortices or dislocations which appear as topological defects in 2d spatial configurations.

## 2. Numerical results and interpretation

The complex Ginzburg–Landau equation (1) was solved using a pseudospectral method with 1024 or 512 modes (for  $L = 1000$  and 500, respectively). The time step ranged from 0.02 to 0.2 with typical run lengths being  $T \sim 10^4$ – $10^5$ .

Fig. 1a,b shows space-time representations of the phase  $\phi(x, t)$  for two typical runs, one in the phase chaos regime and the other in the defect chaos regime. The latter clearly exhibits the defects which appear as space-time dislocations. The average density of defects in  $(1 + 1)$  dimensions was measured by sampling  $\nu(t)$  and recording its jumps  $\nu(t_{n+1}) - \nu(t_n)$ , each one of which is attributed to the occurrence of a defect for some  $x \in (0, L)$  and  $t \in [t_n, t_{n+1}]$ . To avoid systematic undercounting the time sampling was adjusted to keep most  $|\Delta\nu| \leq 1$ . (Note that the probability of occurrence of pairs of defects of opposite sign during an interval  $\Delta t$  decreases with  $\Delta t$ .) The variations of  $n_D$  along several lines in the  $(c_1, c_3)$  plane are shown in fig. 2 and the results are summarized in the phase diagram of fig. 3. While for  $c_1 > c_1^*$  the transition between phase and defect chaos (line  $L_1$  of fig. 3) appears continuous, for  $c_1 < c_1^*$  in the region of  $(c_1, c_3)$  delimited by the lines  $L_2, L_3$ , and  $L_{BF}$  of fig. 3 we found that the two attractors coexist. This means that stationary statistical properties depend on the initial conditions, with hysteretic behavior of  $n_D$  as illustrated in fig. 2. In addition, the defect chaos attractor persists in the BF stable regime<sup>#3</sup>. Near the  $L_1$  line,  $c_3 = \bar{c}_3(c_1)$ , the measured defect density is consistent with  $n_D \sim (c_3 - \bar{c}_3)^2$ , though a subtle question con-

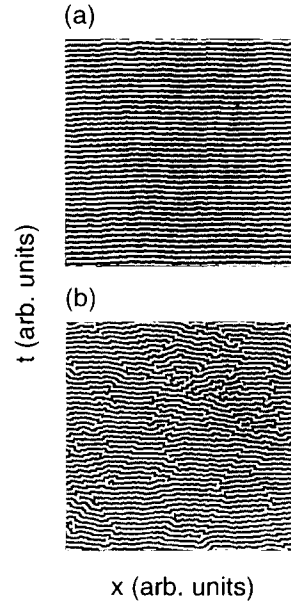


Fig. 1. Lines of constant phase in a space-time plot. (a) Phase chaos regime ( $c_1 = 2$ ,  $c_3 = 0.91$ ). Although the phase fluctuates the lines are continuous. (b) Lines of constant phase in the defect chaos regime ( $c_1 = 2$ ,  $c_3 = 1$ ). The defects appear as space-time dislocations where a constant phase line stops.

cerns discriminating between a continuous transition at  $\bar{c}_3$  (with  $n_D = 0$  in the phase chaos state), and a crossover scenario where  $n_D \neq 0$  but is below our resolution,  $n_D \sim 10^{-6}$ , determined by the length of the run. Our data suggest that  $n_D$  vanishes algebraically at  $\bar{c}_3 > c_3^{BF}$ , rather than persisting into the phase turbulent state, e.g.  $n_D \sim \exp[-(c_3 - c_3^{BF})^{-\alpha}]$ , as might naturally follow from a Gaussian probability distribution for  $\nabla\phi$  (see below)<sup>#4</sup>. We thus interpret  $L_1$  as a continuous transition line and characterize the phase turbulent state by  $n_D = 0$ ,  $\nu(t) = \text{constant}$ .

<sup>#3</sup>For example at the points  $c_1 = 0.4$ ,  $c_3 = 1.5$  and  $c_1 = 0.4$ ,  $c_3 = 1.1$  the defect state was reached by starting in the defect chaos region  $c_1 = 1.3$ ,  $c_3 = 1.5$  and reducing first  $c_1$  and then  $c_3$ . Clearly, because of the finite time of our numerical runs we cannot rule out the possibility that the defect chaotic states in the multiphase regions are long lived transients. Also note that in exploring the phase turbulent region, we have restricted ourselves to the  $\nu = 0$  sector, so there may exist additional chaotic attractors with  $\nu \neq 0$ .

<sup>#4</sup>An exponentially small density of defects would be expected if, for example, their appearance were triggered by the local phase gradient  $|\nabla\phi|$  exceeding some critical value (the width of the corresponding probability distribution being a smooth function of  $c_3 - c_3^{BF}$ ). An example of a simple model for which the defect density becomes exponentially small as a function of a control parameter has been proposed by Huse [10].

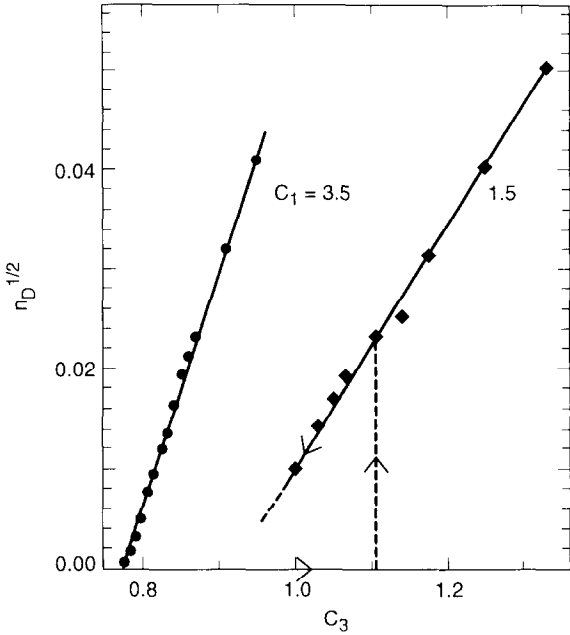


Fig. 2. The defect density along various paths in the  $(c_1, c_3)$  plane. For  $c_1 = 3.5$  the quantity  $n_D^{1/2}$  appears to vanish linearly as  $c_3$  is decreased. For  $c_1 = 1.5$  there is a hysteretic (or “bichaotic”) region  $0.9 \cong c_3 \cong 1.1$  where the value of  $n_D$  depends on initial conditions. The precise behavior of  $n_D$  for  $c_3 < 1.0$  has not been determined.

To further characterize the chaotic states we have evaluated the correlation function of the phase  $\phi$ ,

$$C(x, t) = \langle e^{i(\phi(x,t) - \phi(0,0))} \rangle \equiv \frac{1}{TL} \int_0^T dt' \int_0^L dx' e^{i[\phi(x',t') - \phi(x+x',t+t')]} \quad (2)$$

Similarly we define the gradient correlations

$$g(x, t) = \langle \nabla\phi(x, t) \nabla\phi(0, 0) \rangle, \quad (3)$$

where henceforth the angular brackets have the same meaning as in (2). Fig. 4a shows  $C(x)C(x, 0)$  for 3 points in the defect chaos regime, from which we can extract an exponential correlation length

$$C(x, 0) \underset{x \rightarrow \infty}{\sim} \exp(-x/\xi), \quad (3a)$$

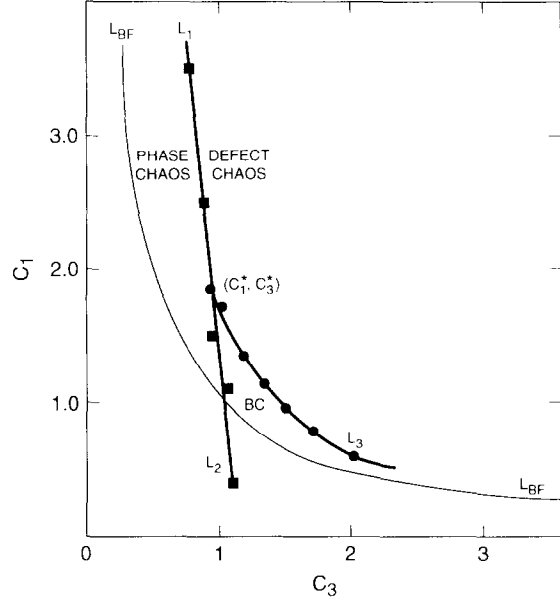


Fig. 3. Phase diagram as determined from the defect density  $n_D$ . The line marked  $L_{BF}$  ( $c_1 = c_3$ ) is the locus of the Benjamin–Feir instability. The defect density is nonzero to the right of the lines  $L_1$  and  $L_3$ . Between the lines  $L_2$  and  $L_3$  below the point  $(c_1^*, c_3^*)$ , there is a bichaotic region (marked BC) where  $n_D$  shows hysteresis i.e. it depends on initial conditions.

which increases dramatically as the line  $L_1$  is approached from the right (see fig. 5). In the phase chaos regime to the left of  $L_1$ , the falloff of  $C(x, 0)$  over the size of the system is not sufficient to allow a direct measurement of  $\xi$  (which if it exists is comparable to or larger than the size of our system,  $L \sim 2^{10}$ ). Instead, we measure a phase diffusion coefficient  $D$  defined by

$$\langle [\phi(x, 0) - \phi(0, 0)]^2 \rangle \sim 2Dx, \quad (4)$$

which is determined by the small- $k$  behavior of the “power spectrum”

$$\hat{g}(k) = \int_{-\infty}^{\infty} dx g(x, 0) e^{-ikx}, \quad (5)$$

shown in fig. 4b. It is seen that  $\hat{g}(k)$  apparently levels off at small  $k$ , to a value  $\hat{g}(0)$  which

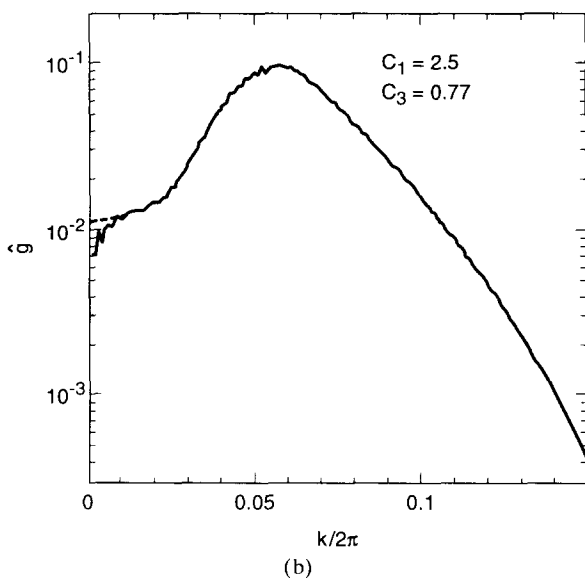
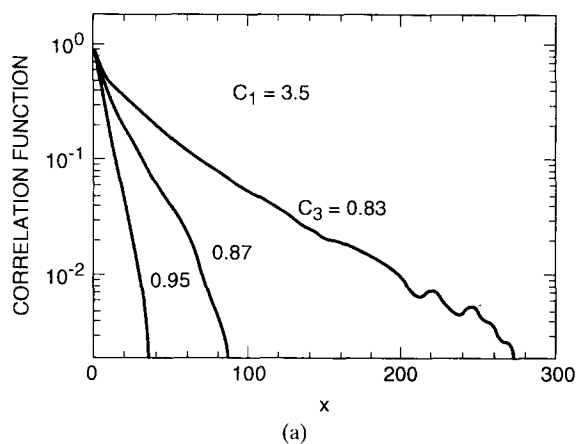


Fig. 4. (a) The equal-time phase correlation function  $C(x)$  in the defect chaos regime near the line  $L_1$ , for  $c_1 = 3.5$ . There is a regime of exponential decay with a correlation length which increases as  $L_1$  is approached. (b) The power spectrum  $\hat{g}(k)$  of the phase gradient correlation function for a point in the phase chaos regime. The dropoff of  $\hat{g}(k)$  for  $k/2\pi \lesssim 10^{-2}$  reflects the incomplete equilibration of the long-wavelength modes during the averaging time. The dashed line was used to estimate  $\hat{g}(k \rightarrow 0)$  for fig. 5.

decreases as one enters the phase turbulence regime, and remains finite and small in that regime as expected from the Kuramoto–Sivashinsky equation [11]. The phase diffusion constant  $D = \frac{1}{2} \hat{g}(k \rightarrow 0)$  is shown in fig. 5. In the

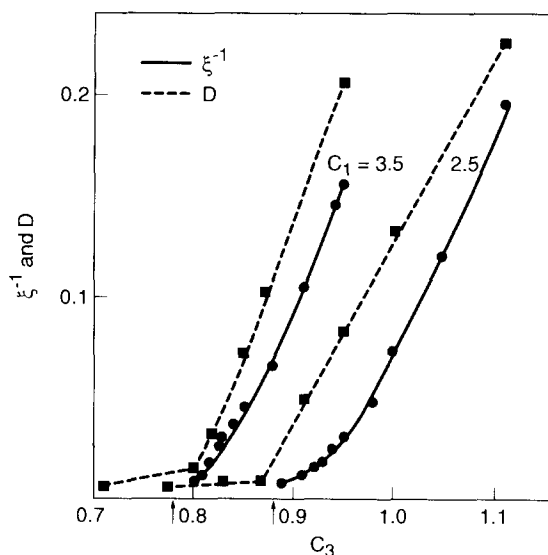


Fig. 5. The correlation length and phase diffusion constant  $D = \frac{1}{2} \hat{g}(k \rightarrow 0)$  along two paths in the  $(c_1, c_3)$  plane. The correlation length is obtained from plots such as the one in fig. 4a and can only be measured in the defect chaos regime to the right of the lines  $L_1$  and  $L_3$  of fig. 3. The diffusion constant is obtained from plots such as the one in fig. 4b, using an extrapolation shown by the dashed line. The arrows on the  $c_3$  scale indicate the values  $\bar{c}_3(c_1)$  on the line  $L_1$  where  $n_D$  vanishes.

phase chaos regime, the relation between  $\xi$  and  $D$  can be derived from the reasonable observation that  $\nabla\phi$  has short spatial correlations, as seen from the behavior of  $g(x, 0)$ . If  $\bar{\xi}$  denotes its correlation length, then for  $|x| \gg \bar{\xi}$ ,

$$\begin{aligned} \phi(x, t) - \phi(0, t) &= \int_0^x \partial_{x'} \phi(x') dx' \\ &= \sum_i \int_{x_i}^{x_i + \bar{\xi}} \partial_{x'} \phi(x') dx' \end{aligned}$$

behaves as a sum of essentially uncorrelated terms and thus leads to a Gaussian distribution [12] of  $\phi(x, t) - \phi(0, t)$ . As a consequence one obtains

$$\begin{aligned} C(x) &= \langle e^{i[\phi(x,0) - \phi(0,0)]} \rangle \\ &\approx \exp\left\{-\frac{1}{2} \langle [\phi(x,0) - \phi(0,0)]^2 \rangle\right\} = e^{-Dx}. \end{aligned} \tag{7}$$

In the defect regime we expect extra contributions to phase diffusion from the  $2\pi$  jumps of the phase across the defects, which would not contribute to the decay of  $C(x)$ . Thus we expect in general

$$\xi^{-1} \leq \frac{1}{2} \hat{g}(0) = D, \tag{8}$$

with the equality holding in the phase chaos regime. The data in fig. 5 are not inconsistent with (8), although the equality could not be tested.

The different regimes also differ in their time correlations, with the correlation function  $C(t) = C(x=0, t)$  falling off exponentially in the defect turbulent regime. The correlation time  $\tau$  increases dramatically as  $L_1$  is approached from the right, roughly as  $\tau \sim (c_3 - \bar{c}_3)^{-2}$  (see fig. 6). The exponent 2 is anticipated if one makes the reasonable assumption that the exponential decay of the temporal correlation function is dominated by defects; then the correlation time is expected to be comparable to the average time

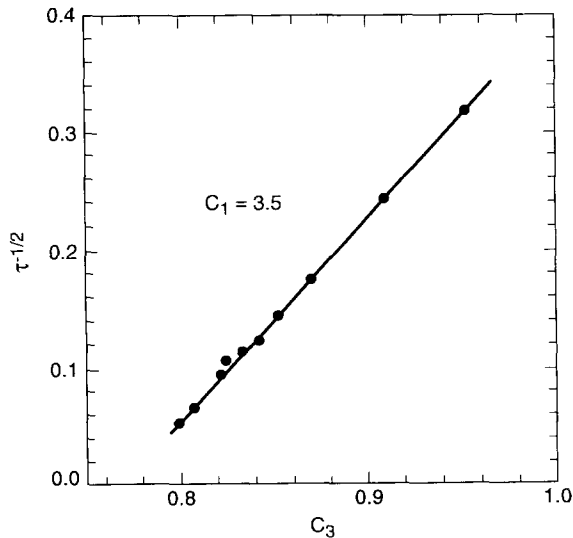


Fig. 6. The correlation time for the temporal correlation function  $C(x=0, t)$  along a line in the  $(c_1, c_3)$  plane. The time appears to diverge quadratically as  $L_1$  is reached.

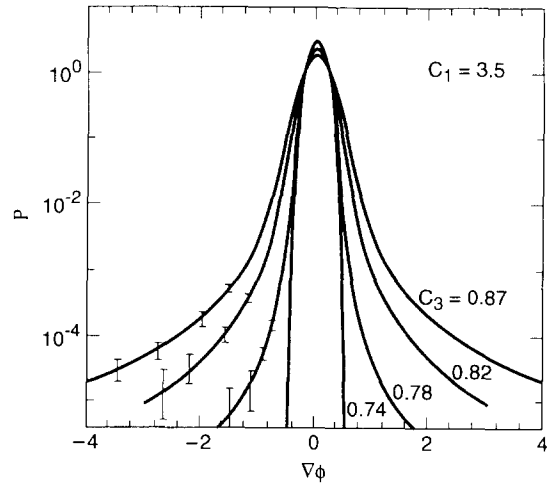


Fig. 7. The probability distribution function of the phase gradient  $P(\nabla\phi)$  for various points near  $L_1$  with  $c_1 = 3.5$ . In the phase chaos regime ( $c_3 = 0.74$ ) the distribution is asymptotically Gaussian, while in the defect regime the distribution falls off slower than exponentially.

between the appearance of two defects near the measurement point. Hence, one has  $\tau^{-1} \sim n_D \sim (c_3 - \bar{c}_3)^2$ . On the other side of  $L_1$  we have observed long transients in the relaxation of the long-wavelength modes (e.g. in the  $\hat{g}(k)$  spectrum for  $k \approx 2\pi/L$ ), suggesting the existence of diffusive or subdiffusive [13] modes in the phase turbulent regime and possibly algebraic falloff of  $C(t)$ . However, as with the spatial dependence of  $C(x, 0)$ , the falloff of  $\hat{C}(k, t)$  with time for  $k \ll 1$  was too slow to allow a conclusive determination of the asymptotic behavior.

Finally, we have also measured the probability distribution of the phase gradient, anticipating that it could affect the likelihood for the appearance of defects<sup>#4</sup>. In fig. 7 we show the probability  $P(\nabla\phi)$  obtained from a sequence of configurations in steady state, for various points on either side of the line  $L_1$ . On the logarithmic scale of the figure a Gaussian is a parabola, so we see that the distribution is reasonably Gaussian for large fluctuations in the phase turbulence regime, while in the defect regime the distribution falls off slower than exponentially.

### 3. Discussion and conclusion

We have carried out a numerical simulation of the one-dimensional complex Ginzburg–Landau equation (1) on a large interval, in order to develop means of quantitative characterization of extensive chaos. We have found two distinct chaotic phases, “defect chaos” characterized by the presence of space-time defects, fluctuations of the winding number and exponential decay of temporal correlations, and “phase turbulence” with apparently constant winding number, a vanishing density of defects, and slower than exponential decay of temporal correlations. Although we have observed substantial equal-time spatial correlations on the length scale of our system in the phase turbulent state, we have argued in favor of exponential decay of  $C(x)$  on the basis of the proposed relation between the inverse correlation length  $\xi^{-1}$  and the phase diffusion constant  $D$  (both of which turn out to be numerically small for the values of  $c_1, c_3$  considered). If one extends this argument to higher dimensions, assuming that the small- $k$  behavior of the gradient correlation function  $\hat{g}(k)$  is unchanged [i.e.  $\hat{g}(k \rightarrow 0) = 2D$ ] one obtains

$$\langle [\phi(x, 0) - \phi(0, 0)]^2 \rangle \sim x^{2-d} + \text{const.} \quad (9)$$

The correlation function  $C$  thus goes as a power law for  $d=2$ , and shows long-range order for  $d=3$ , a familiar result from equilibrium systems with  $O(2)$  continuous symmetry [14]. In that case the diffusion constant  $D$  (for  $d=1$ ) or the power law exponent (for  $d=2$ ) are proportional to the temperature  $T$ , whereas in our case we have a chaotic state and we have assumed that the width of the distribution of  $\nabla\phi$  plays the role of temperature. These considerations, however, deal only with the spatial dependence of the equal-time correlations and shed no light on their temporal behavior. On the other hand, the suppression of defects in the phase chaos regime is surprising, especially from the statistical point of

view based on stationary distributions. If true, the defect “suppression” must be of dynamical origin. A study of the dynamic correlation functions (and of suitable response functions) is a necessary next step towards the “statistical mechanics” of extended chaotic systems [2]. An obvious question is whether our phenomenological discussion of the phase turbulent state in terms of a Gaussian  $P(\nabla\phi)$  is correct. Why is the diffusion constant  $D = \xi^{-1}$  so small in the phase chaos regime? Can one develop a theory describing both static and dynamic correlations in terms of statistical mechanics in  $(d+1)$  (i.e.  $1+1$ ) dimensions, as proposed by Bunimovich and Sinai [15] for a particular coupled map system?

Although the phase diagram and characterization of phases we have obtained seem to be a good first approximation, many other questions are left unanswered. Will our description of the phase turbulent state, and the identification of the transition to the defect chaos regime hold up in the asymptotic large system and long time limit? A careful further study of finite-size and finite-time effects on the defect density and correlation functions is required to rule out (and/or understand) a possible smooth crossover between the phase and defect regimes. Of particular interest here is the possibility of an exponentially small density of defects in the phase turbulent regime (below the resolution of the present study). It would also be desirable to calculate the temporal correlation function more accurately since we expect it to exhibit a change from exponential to algebraic decay [13] across the  $L_1$  line; this would allow the correlation time to be interpreted as a disorder parameter for the transition. In addition, further calculations are needed to fully map out the phase diagram of eq. (1). For example, what is the behavior in the  $\nu \neq 0$  sectors of the phase chaos regime [7]<sup>#5</sup>. Also, there are preliminary indications that in the limit  $c_1 \rightarrow 0$  (over a range of  $c_3$ ) there are

<sup>#5</sup>For  $\nu \neq 0$  we have also observed traveling pulse-trains, see ref. [16].

slow time scales in the system and possibly a “freezing” transition leading to a state with long-range temporal correlations but only short-range spatial order. Another interesting regime is  $c_1, c_3 \rightarrow +\infty$  i.e. the approach to the nonlinear Schrödinger equation, where some analytic progress might be possible. The other quadrants of the  $(c_1, c_3)$  plane<sup>#1</sup>, as well as higher-dimensional systems [17] for all  $c_1$  and  $c_3$  also merit further study, since qualitatively different phenomena are expected to appear (true “amplitude” chaos, long-range order, topological defects, “wave collapse”, etc).

Finally, an important issue concerns the experimental relevance of our results. It has been noted that the variant of eq. (1) valid for a subcritical bifurcation [5] might be a model for chaos in binary-fluid convection [18], and other systems with traveling waves may also be represented by this model. It would be interesting to have experimental determinations of  $n_D$  and of the correlation functions  $C(x, t)$  and  $g(x, t)$ .

### Acknowledgements

The authors acknowledge discussions with D. Bensimon, V. Croquette, M.C. Cross, D.A. Huse, P. Kolodner, and E.D. Siggia. A. Pumir was supported in part by the Air Force Office of Scientific Research under grant #91-0011.

### References

- [1] B.-L. Hao, Chaos (World Scientific, Singapore, 1984).
- [2] P.C. Hohenberg and B.I. Shraiman, *Physica D* 37 (1989) 109.
- [3] See e.g. M.C. Cross and P.C. Hohenberg, *Rev. Mod. Phys.* (to be published).
- [4] C.S. Bretherton and E.A. Spiegel, *Phys. Lett.* 96 A (1983) 152.
- [5] W. Schöpf and L. Kramer, *Phys. Rev. Lett.* 66 (1991) 2316.
- [6] T.B. Benjamin and J.E. Feir, *J. Fluid Mech.* 27 (1967) 417;  
J.T. Stuart and R.C. DiPrima, *Proc. Roy. Soc. London* A362 (1972) 27.
- [7] B. Jانياud, A. Pumir, D. Bensimon, V. Croquette, H. Richter and L. Kramer, *Physica D* 55 (1992) 269.
- [8] Y. Kuramoto and T. Tsuzuki, *Prog. Theor. Phys.* 55 (1976) 356;  
G.I. Sivashinsky, *Acta Astronaut.* 4 (1977) 1177.
- [9] H. Sakaguchi, *Prog. Theor. Phys.* 83 (1990) 169; 84 (1990) 792.
- [10] D. A. Huse (unpublished).
- [11] Y. Pomeau, A. Pumir and P. Pelce, *J. Stat. Phys.* 37 (1984) 39.
- [12] A. Pumir, *J. Phys. (Paris)* 46 (1985) 511.
- [13] S. Zaleski, *Physica D* 34 (1989) 427.
- [14] T.M. Rice, *Phys. Rev.* 140 (1965) 1889.
- [15] L.A. Bunimovich and Y.G. Sinai, *Nonlinearity* 1 (1988) 491.
- [16] See A. Pumir, B.I. Shraiman, W. van Saarloos, P.C. Hohenberg, H. Chaté and M. Holen, in *Ordered and Turbulent Patterns in Taylor–Couette Flow*, ed. C.D. Andereck and F. Hayot (Plenum, New York, 1992).
- [17] P. Szépfalussy and T. Tél, *Physica A* 112 (1982) 146;  
M. Bartucelli, P. Constantin, C.R. Doering, J.D. Gibbon and M. Gisselält, *Physica D* 44 (1990) 421.
- [18] P. Kolodner, J.A. Glazier and H. Williams, *Phys. Rev. Lett.* 65 (1990) 1579.